

From river flow to spatial flow: flow map via river flow directions assignment algorithm

Zhiwei Wei, Su Ding, Yang Wang, Yuanben Zhang, Wenjia Xu

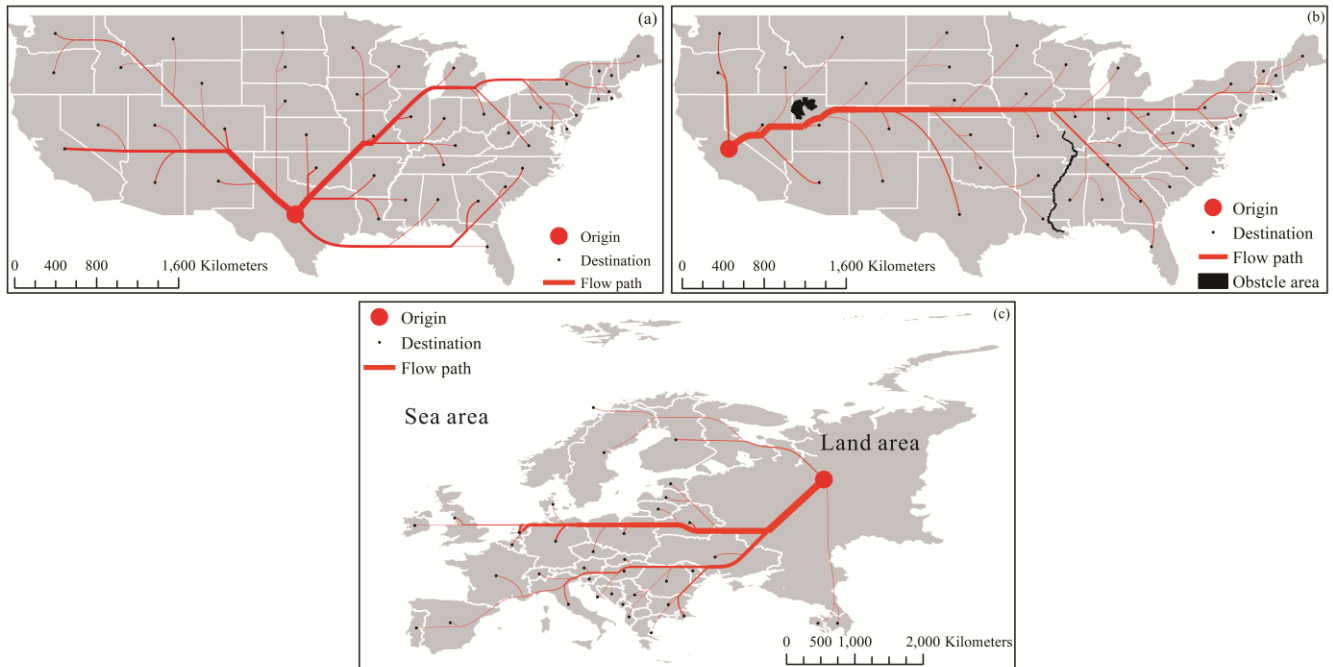


Fig. 1. Flow maps generated by proposed approach. (a) Migration from Texas to other states in 2000 US Census; (b) Migration from California to other states in 2000 US Census considering obstacle areas; (c) Good exports from Russia to other European countries ($\geq 0.01\%$) in 2019 in which sea areas are avoided as much as possible.

Abstract—Flow map is an effective way to visualize object movements across space over time. It aims to model the paths from destinations to origins with quality constraints satisfied, which is similar to river system extraction in a digital elevation model (DEM). In this paper, we present a novel and automated approach called RFDA-FM for spatial flows from one origin to multiple destinations using a river flow directions assignment algorithm in DEM. The RFDA-FM first models the mapping space as a flat surface by DEM. An improved maze solving algorithm (MSA) is then introduced to assign the flow directions by constraining its searching directions, direction weights and searching range. The paths from the destinations to the origin are obtained iteratively based on the improved MSA according to the path importance. Finally, these paths are rendered with varied widths and smoothed according to their volume using the Bézier curves. The evaluation results indicate that the flow maps generated by RFDA-FM can have a higher quality with uniform distribution of edge lengths and avoidance of self-intersections and acute angles by comparing to the existing approaches. The experiments demonstrate that RFDA-FM is also applicable for heterogeneous mapping space or mapping space with obstacle areas.

Key words: Flow map; automatic cartography; hydrology model; maze solving algorithm; DEM.

1 INTRODUCTION

Since the first flow map introduced by Henry Drury Harness in 1837 [1], it has been a long history to depict migration patterns, movement of goods, knowledge, disease or animals with a flow map due to its effective reduction of visual clutter and clear insight on the spatial distribution of moving phenomena [2]. With the rapid development of information technology in past several decades, it has made the global economy and society more open and networked [3]. Movements across regions become easy

- Zhiwei Wei and Yang Wang are with Aerospace Information Research Institute, Chinese Academic of Sciences and Key Laboratory of Network Information System Technology (NIST), Aerospace Information Research Institute, Chinese Academy of Sciences. E-mail: 2011301130108@whu.edu.cn Primular@163.com.
- Yuanben Zhang and Wenjia Xu are with Aerospace Information Research Institute, Chinese Academy of Sciences, Key Laboratory of Network Information System Technology (NIST), Institute of Electronics, Chinese Academy of Sciences and School of Electronic, Electrical and Communication Engineering, University of the Chinese Academy of Sciences. E-mail: zhangyb@aircas.ac.cn, xuwenjia16@mails.ucas.ac.cn.
- Su Ding is with the College of Environmental and Resource Science, Zhejiang A & F University. E-mail: suding@zafu.edu.cn.

and frequent. Mapping these flows across regions over time nowadays is getting more and more important and has been a central task in graph visualization.

Many approaches have been proposed to map flow data related to different number of origins, flow forms or mapping spaces [4]. For example, Guo and Zhu [5] introduced a many-to-many flow map approach for taxi trips with GPS locations. While Yang et al. [6] explored the usability of 2D and 3D flow Maps in immersive environment. Because flow maps aim to express spatial distribution of moving phenomena with reduction of visual clutter, strategies including hierarchical clustering, data aggregation, edge bundling, edge routing, force directed algorithm, spatial tree-map and matrix-based techniques have also been introduced [5, 7-12]. Due to the numerous innovative approaches of flow maps, we here restrict our attention on the flows from one origin to multiple destinations. It is also known as a so-called one-to-many flow maps and has been widely used as a tree layout [7]. The trunks and branches of the layout are generated by bundling edges into hierarchical levels and rendered with varied widths to delineate the flow routes and volumes [13].

To automate the production of a one-to-many flow map, approaches including spiral tree based and force-directed based approaches have been proposed [2, 13-15]. But these approaches may suffer from problems such as low degree of automation or high computational cost. For example, approach of Debiassi et al. [15] requires many manual interventions; while approach of Verbeek et al. [2] performs a global optimization which is time-consuming. And approach of Sun [13] needs a series of additional cartographic operations including edge simplification, straightening, smoothing and rendering. Furthermore, current flow map approaches lack generalization ability, i.e., different approaches need to be designed for varied purposes, which is hard to apply for different occasions, e.g., varied mapping spaces. It is necessary to develop a relatively efficient and unified model to automate the production process. The river system, as natural flows across geographical regions can be considered as a special kind of flow map. Many approaches have been proposed and used in hydrological applications to extract river system based on a digital elevation model (DEM) [16]. If the mapping space is modelled as a DEM data, the one-to-many flow map can also be produced using hydrological model which is applied to extract river system in hydrological applications. As mapping space of a flow map is usually considered as uniform, the approach to extract river system over flat surfaces in DEM can be applied.

Motivated by the above thoughts, we proposed an approach named RDFA-FM to produce the one-to-many flow map using river flow directions assignment algorithm over flat surfaces in DEM. First, the RDFA-FM models the mapping space as a flat surface by DEM. The varied mapping spaces, i.e., mapping space with obstacle areas or heterogeneous mapping space can all be modelled as properties of the DEM data. Second, the maze solving algorithm (MSA) widely used to assign river directions in hydrological applications is applied to decide the flow direction. The MSA is improved by constraining its searching directions,

direction weights and searching range according to the quality constraints involving in production of flow maps. The flow paths from all destinations to the origin are obtained iteratively based on the improved MSA according to the path importance by considering their length. Third, we smoothly render the flows with varied widths by flow accumulation using the Bézier curves.

The rest of the paper is organized as follows. Section 2 presents the-state-of-the-arts approaches on one-to-many flow maps and introduces river flow directions assignment algorithms over flat surfaces in DEM. Section 3 illustrates the methodology of RDFA-FM. Section 4 evaluates the RDFA-FM, compares with previous works and discusses strategy effectiveness and parameter settings in RDFA-FM. Section 5 concludes the paper and identifies issues for future work.

2 RELATED WORKS

2.1 One-to-many flow maps

2.1.1 Definitions

To achieve a better illustration of proposed approach, some definitions are given as follows (Figure 2). The one-to-many flow map is with a tree layout connecting destinations and the origin and can be represented as a graph: $G=(V,E)$, where V represents the nodes set of the flow map, E represents the edges connecting two nodes in V , and $e_i \in E$ can be a curve or a straight line. The objects flow along the edges from the destinations to the origins, as shown in Figure 2.

Origin node (On): The node represents the origin, e.g., node A.

Destination node (Dn): The node represents a destination, e.g., nodes D, F, H, I and J.

Flow in node (Fn): The intersection node of two edges, e.g., nodes B, C, E and G.

Hang edge (He): The edge connects a Dn and a Fn , e.g., edges DB, FE, HE, IG and JG.

Non-hang edge (NHe): The edge connects two Fns or the On and a Fn , e.g., AB, BC, CE and CG.

Path (Fp): The route from a node to another, e.g., JGCBA is a path from destination node J to the origin node A.

Edge volume (Ev): The amount of movement objects flow along the edge; Ev of an He is the amount of movement objects from the On to its corresponding Dn , e.g., 100 for edge HE; Ev of an NHe is the sum of Ev of its all flow in edges, e.g., 280 for edge CG.

Flow in angle (Fa): The angle between a He and its connecting NHe which is with the largest Ev , e.g., angle ABD.

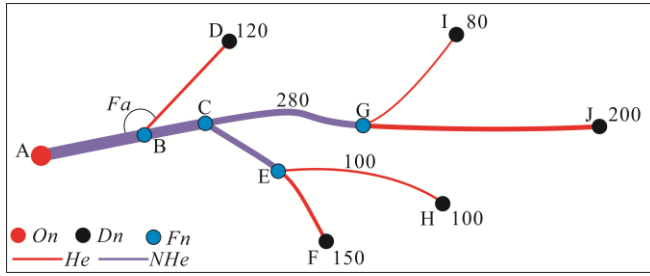


Fig. 2. Definitions on the flow map.

2.1.2 Quality constraints

Requirements of a flow map are usually developed into constraints to rule its production [17]. Different constraints have been developed for different purposes. For example, Debiassi et al. [15] suggested five constraints including cross-free of edges, minimum overlaps between nodes and edges, etc. While Jenny et al. [9] analyzed the design principles for origin-destination flow maps with user study and eight kinds of constraints on graph length, symmetry, etc. are proposed. Dong et al. [18] analyzed the influence of smoothness and thickness of the flow paths using eye tracking experiments. To evaluate these constraints, measures such as the total length of the flow map, the number of edge-crossings, and the number of acute Fa , visual smoothness index, etc. are proposed [13,19,20]. Though different constraints have been proposed, they share many common properties. We summarize the constraints involving in production of the one-to-many flow map as follows, particularly according to Verbeek et al. [2], Sun et al. [13] and Jenny et al. [17].

(1) Geometry

Type (GC₁): Curved edges are preferred than straight edges in a flow map, and an edge is more likely to be rendered as a curve if possible [17, 18].

Total Length (GC₂): Larger total length of the flow map means larger visual burden, and needs to be minimized [2].

(2) Relation

Acute flow in angle (RC₁): Acute flow in angles (Fa) may have negative impact on response time, and need to be avoided as much as possible [21, 22].

Edge crossing (RC₂): Edge crossings may lead to a confusion, and need to be avoided as much as possible [15].

Overlap between nodes and flow paths (RC₃): Overlap between nodes and flow paths may lead to a visual clutter, and need to be avoided as much as possible [13].

Crossing between flow paths and important map objects (RC₄): Some map objects may be important and the flow paths need to avoid these important map objects to aid recognizability [2].

(3) Distribution

Length uniform for hang edges (DC₁): Hang edges (He) need to have similar length for an aesthetics purpose [15, 23].

Symmetric arrangements (DC₂): A symmetric layout is preferred to asymmetric layout, and the flow map need to be symmetric as much as possible [17].

Thickness arrangement (DC₃): Edge widths of the flow map should be drawn atop thick ones to the thin ones [2].

2.1.3 Algorithms

The earliest one-to-many flow map can be traced back to Henry Drury Harness in 1837 [24]. Shortly after, Charles Joseph Minard extended this idea to depict economic topics such as import or export of wine, cotton and coal [21]. While these early flow maps are most drawn by hands, Tobler [25] first introduced an automatic system to produce flow maps. But in his approach, straight lines are drawn from destinations to the origin with varied widths and colors. It will result in visual clutter, which has been the main concern in later developed approaches.

To overcome this problem, Tobler [25] introduced a filtering strategy. This strategy is also adopted by Elzen and van Wijk [26] in interaction between flow maps. As an important strategy to reduce visual clutter in graph visualization, edge bundling is also applied for flow map. Phan et al. [7] proposed an algorithm to bundle edges based on the hierarchical clustering. But the approach may not smooth all paths and have a large total graph length. Debiassi et al. [15] used the force directed algorithm to bundle edges with node merge and node move. But it is a supervised approach and some manual interventions are required. Steiner tree, as a graph connects a set of points with minimum total length by using extra points, is also widely used in flow map [27]. Verbeek et al. [2] introduced a spiral tree by restricting the angle of a Steiner tree to produce smooth and crossing-free flow map. Nocaj and Ulrik [14] introduced a stub bundling strategy based on the spiral tree. While Sun [13] produced the one-to-many flow map with triangulation, approximate Steiner trees, and path smoothing. In these Steiner tree-based algorithms, the first approach is time consuming for it needs a global optimization [2]. The third approach requires a series of cartographic operations, including simplification, straightening, smoothing which may be not easy-to-use [13]. With the development of the augmented-reality technology, the usability of 2D and 3D flow Maps in immersive environment is also explored [6].

Some researchers also discuss the taxonomy which may involve the flow map. For example, flow map can be considered as a kind of geospatial network. Schöttler et al. [4] give a detailed taxonomy for visualization of geospatial network including the representation of geographical information, network information and use of interaction. As flow maps aims to reduce visual clutter via edge bundling, Zhou et al. [8] reviewed the cost-based, geometry-based, and image-based in edge-bundling approaches, in which flow maps are also included. According to the number of origins, flow maps can also be classified into many-to-many and one-to-many layouts [13].

2.2 River flow directions assignment algorithm over flat surfaces in DEM

2.2.1 Process

River flow extraction in DEM is the key technology in digital watersheds, hydrological analysis, and soil erosion analysis [16]. An automatic extraction of the river flows usually contains four steps: (1) depression filling; (2) flow direction calculation; (3) flow accumulation; (4) flow track

based on the flow direction with defined flow accumulation thresholds [28]. As the elevation in a flat surface is the same, depression filling is not performed in river flow extraction. Among the remaining three steps, flow direction calculation is the basis for subsequent two steps. Flow accumulation and flow track can be easily performed with a good calculation of flow direction.

2.2.2 Algorithms

Flow direction calculation is the basis for flow accumulation and flow track. Thus, flow extraction algorithms over flat areas in DEM mainly aim to calculate the flow directions. These algorithms can be categorized into two types: effectiveness first or efficiency first.

Effectiveness first algorithms aim to improve the accuracy of flow direction calculation. By increasing the elevation of grid cells, Jenson and Domingue [28] assigned flow directions in flat area by increasing the elevation from the outlet. But this approach may generate parallel flows. By decreasing the elevation of the grid cells, Garbrecht and Martz [29] calculated flow directions by adding a gradient from higher grids to lower grids. As it can produce flow paths which are in line with actual situation, approaches to improve it have also been proposed by Soille et al. [30], Zhang and Huang [31], Barnes et al. [32] and Liu et al. [33]. Another basic idea for flow direction calculation is to obtain flow paths according to their importance iteratively. Tribe [34] extracted flow directions in flat area by assuming the main flow path was a straight line from inlet to outlet. Other flow paths were then decided iteratively by connecting to their nearby earlier generated flow paths. As for not all paths are exactly straight lines, Zhang et al. [35] improved the approach by introducing a maze solving algorithm (MSA) to decide the flow directions.

Efficiency first algorithms aim to reduce the computational cost and mainly involves the strategies to reduce or speed up the calculation. For example, Zhu et al. [36] applied a neighbor-grouping scan loop strategy. While Wang and Liu [37] presented a priority-flood algorithm which processed depressions from the edge grid cells to the interior cells. These strategies help reduce the computation complexity. Barnes et al. [38] applied different increments to flat cells in masked DEMs to avoid iterative calculation. Su et al. [39] integrated depression filling and direction assignment with a chain code matrix based on Barnes et al.'s algorithm. Their approach guides the calculation of the gradient directly from higher terrain towards lower terrain instead of applying iterative searching. And a distance transform was also later introduced to speed up the searching process by themselves [40]. And Yu et al. [41] used a "first-in, first-out" queue to process depressions and flat area and a priority queue to process other

areas which can effectively reduce the computation complexity.

3 METHODOLOGY

3.1 Framework

According to the river flow extraction process over the flat surfaces in DEM illustrated in Section 2.2.1, the proposed approach (RFDA-FM) to produce a the one-to-many flow map consists of three steps (Figure 3).

Step 1: Modelling the mapping space as a DEM data: The mapping space is modelled as a DEM data over flat surface. The destinations and the origin are represented by their corresponding grids. The destination grids are considered as grids with an outflow whose flows eventually gather in the origin grid.

Step 2: Flow direction calculation: An improved maze solving algorithm (MSA) is introduced to assign the flow directions to obtain the flow path from a destination to the origin. The flow paths from all destinations to the origin are obtained iteratively according to the path importance, which is defined by their length.

Step 3: Flow render based on flow accumulation: The volume of each edge in the flow map is calculated with flow accumulation. The edges are then rendered smoothly with varied widths using the Bézier curves according to their volume.

we will illustrate each step in details and present our approach in the following sections.

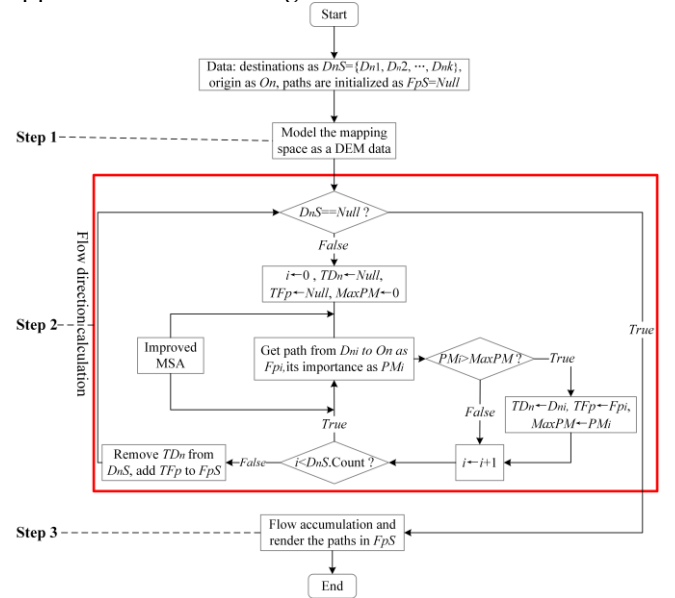


Fig. 3. Framework.

3.2 Step 1: Modelling the mapping space as DEM data

DEM is a representation of the elevation in a continuous terrain surface via irregular or regular grids with a certain resolution [42]. The mapping space of a flow map is usually considered as uniform, and is modelled as flat surface with DEM by defining the grid type, resolution and range.

Suppose the origin and destinations as a node set $PS = \{O_1, D_2, \dots, D_n\}$, where O_1 is the origin and D_n is a des-

tionation; the regions as a based map denoted as $RegS = \{S_1, S_2, \dots, S_n\}$. D_n has a property as V_n , which represents the flow volume from O_1 to D_n . The mapping space is modelled as a DEM data over flat surface as follows (Figure 4).

(1) **Grids**: Regular grid (square) is adopted considering its lower computational cost and common uses (Figure 4).

(2) **Resolution**: The resolution needs to promise that the closest points in PS do not fall into the same grid. But a higher resolution requires a higher computational cost. According to the detailed analysis of resolution setting in spatial applications of point samples by Hengl [43], the resolution (R_s) of the DEM is set considering the shortest distance between points in PS as Equation (1).

$$R_s = \frac{AveMinD_{(5\%)}}{4} \quad (1)$$

Where $AveMinD_{(5\%)}$ is the average distance between the first 5% closest point pairs in PS .

(3) **Range**: The range of DEM data can be set according to the envelope of $RegS$ or PS , e.g., the range is set as the envelope of $RegS$ in Figure 4. While the range is set according to the envelope of PS , the range need to be set by extending a half grid out based on the envelope of PS to avoid points in PS locating on the boundary.

(4) **Consideration of obstacle area**: The flow paths from destinations to the origin may sometimes need to avoid obstacle area [2]. For example, areas with bad weather may need to be avoided while mapping the movement of goods. Thus, grids within these areas need to be deleted from existing range, e.g., the grids colored red in Figure 4. Based on the similar idea, point, linear, or planar obstacle areas can all be represented by deleting corresponding grids in our approach, as shown in Figure 4.

(5) **Consideration of heterogeneous mapping space**: Differences between areas may sometimes be considered. For example, bypassing the land may have a higher travel cost than the sea while mapping the flow of goods. Two strategies can be applied for different areas as does in DEM data [30]: 1) Different areas can be represented as grids with different types, as shown in Figure 4, the areas within $RegS$ are represented as Type 2 grid, while the other areas are represented as Type 1 grid; 2) Different areas can also be represented as grids with varied resolutions.

With the above definitions, the mapping space is then modelled as a DEM data over flat surface. Each point in PS can be considered as a grid in the DEM. The destinations are considered as grids with outflow whose flows eventually gather in the origin grid.

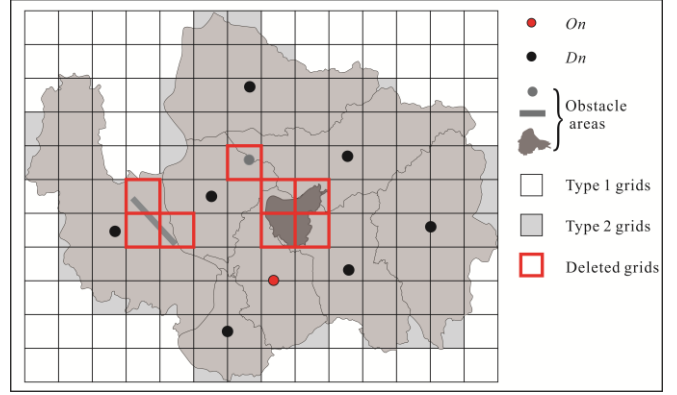


Fig. 4. Modelling the mapping space as a DEM data.

3.3 Step 2: Flow direction calculation

Flow direction calculation from grid A to B means compute the path from grid A to B. According to Tribe [34], the flow path from the destination grid to the origin grid is defined as a path with the shortest length in a DEM data and usually obtained with a maze solving algorithm (MSA). Thus, an improved MSA is introduced to obtain the shortest path from a destination grid to the origin grid in a flow map after the mapping space is modelled as a DEM data. All paths from all destination grids to the origin grid in the flow map are then generated iteratively with the improved MSA according to the path importance. Three keys are involved in flow direction calculation: (1) Path length definition; (2) Improved MSA; (3) Path importance definition.

3.3.1 Path length definition

Path length (PL) can be computed according to their flowing through grids. The distance (D_{cn}) between two adjacent grids is defined first. The PL is then defined based on D_{cn} by considering constraints GC_2 , RC_1 and DC_1 .

The paths from the destination grids to the origin grid are generated iteratively in our approach. Suppose the earlier generated paths as $FpS = \{Fp_1, Fp_2, \dots, Fp_n\}$, given a destination grid (DG_i), a potential path ($cacheFp_i$) from DG_i may flow in any grid of FpS to the origin grid (OG). The definitions are given as follows.

(1) Distance between two adjacent grids

Grids may have different types and can be assigned different weights in distance definition. The D_{cn} is defined as Equation (2), Figure 5(a).

$$D_{cn} = \begin{cases} 0.5R_s \times \delta_i + 0.5R_s \times \delta_j & \text{(Orthogonal neighbors)} \\ \sqrt{2} \times (0.5R_s \times \delta_i + 0.5R_s \times \delta_j) & \text{(Diagonal neighbors)} \end{cases} \quad (2)$$

Where R_s is the resolution of the DEM data, defined in Section 3.2, δ_i and δ_j are the weights considering the grid types and are set by users. If the mapping space is considered as homogeneous, grids are all the same type and $\delta_i = \delta_j = 1$.

(2) Path length definition considering GC_2

If $cacheFp_j$ flow in a grid of FpS , it can be divided into $sub-Fp_j^1$ and $sub-Fp_j^2$, and $sub-Fp_j^2$ is a sub-path of $Fp_n \in FpS$. As shown in Figure 5(a), the path from the destination grid B may flow in path ADO at grid c_1 or c_2 to the origin grid O. On these occasions, paths C_1O or C_2O

are parts of an earlier generated path. Thus, the $sub-Fp_j^i$ is not a newly generated path which help minimize the total length of the flow map (GC_2). Thus, the path length (PL_j) of $cacheFp_j$ is defined by considering GC_2 as Equation (3).

$$PL_j = subPL_j^1 + subPL_j^2 \times \omega \quad (3)$$

Where $subPL_j^1$ and $subPL_j^2$ are length of $sub-Fp_j^1$ and $sub-Fp_j^2$, ω is a weight and $\omega \leq 1$.

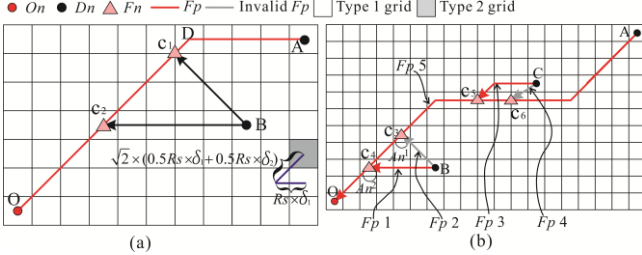


Fig. 5. (a) Path length definition; (b) Path length refinements considering constraints RC_1 and DC_1 .

(3) Path length refinements considering constraints RC_1 and DC_1

The flow path from the destination grid to the origin grid is defined as a path with the shortest length [34]. For the given DG_i , any path ($cacheFp_j$) from DG_i flow in a grid of FpS to the origin grid (OG) can be a candidate flow path from DG_i to OG. If $cacheFp_j$ violates a constraint defined in Section 2.1.2, a penalty strategy is applied for the PL_j of $cacheFp_j$, then $cacheFp_j$ is less likely to be the shortest flow path from DG_i to OG, as Equation (4).

$$PL_i = PL_i + PL_{pen} \quad (4)$$

PL_{pen} is a large constant and set as $PL_{pen} = 20R_s$ in this approach. Constraints including RC_1 and DC_1 are considered in the penalty strategy.

Refinement considering RC_1 : RC_1 rules that acute flow in angles (Fa , defined in Section 2.1.1) need to be avoided. Acute Fa is defined by setting a threshold (T_a): If $Fa \leq T_a$, then Fa is an acute one. If Fp_i flows in $Fp_n \in FpS$ with an acute Fa , then the penalty strategy is performed for Fp_i . As shown in Figure 5(b), Fp_5 is an earlier generated flow path from destination grid A to the origin grid O. To obtain the flow path from destination grid B to the origin grid O, each grid of Fp_5 can be a candidate flow in location. But the Fa (An^1) is an acute angle if Fp_2 flows in Fp_1 at grid c_1 . Then Fp_2 is penalized by Equation (4) and the Fp_1 is finally obtained as the shortest path from destination grid B to origin grid O for the Fa (An^2) at the flow in grid c_2 isn't an acute one.

Refinement considering DC_1 : DC_1 rules that hang edges (He , defined in Section 2.1.1) need to have similar length. It can be satisfied to some extents by setting a minimum threshold (T_d) for length of He . If a flow path (Fp_i) flows in $Fp_n \in FpS$ and an He^i is then made, length of He^i denoted as PL_{sub}^i : if $PL_{sub}^i \leq T_d$, the penalty strategy is performed for Fp_i . As shown in Figure 5(b), Fp_5 is an earlier generated flow path from destination grid A to the origin grid O. Fp_3 and Fp_4 can both be considered as the flow paths from destination grid C to the origin grid O. If T_d is set as $T_d = 2\sqrt{2}R_s$, then Fp_4 is penalized by Equation (4). The Fp_3 is the finally obtained as the shortest path from destination grid C to origin grid O for it meets DC_1 .

3.3.2 Improved maze solving algorithm

Maze solving is a classical problem in graph theory and data structure fields. As it aims to find the shortest path between the entrance to the outlet in a given labyrinth, which has been applied to generate flow direction in DEM successfully [35]. The flat surface is considered as labyrinths without inside walls, the destination grid is considered as an entrance and the origin grid is considered as an outlet.

Three definitions are required in a maze solving algorithm (MSA): searching directions, direction weights and searching range [44]. The searching directions determine the potential directions to be searched; the direction weights determine which direction is prior to be searched; the searching range determines where can be searched. They need to be defined according to the requirements of flow map production.

(1) Searching directions

As a grid in DEM, its outflow direction to its neighborhood grids can be 8 directions (8D), denoted as $8D = \{0, 1, 2, 3, 4, 5, 6, 7\}$ [45]. But it is time consuming if all directions are explored each time. It may be more suitable to only search in the directions towards the target grid, but not search all directions. For example, the searching directions may be $\{0, 1, 2\}$ while searching from destination grid A to a target grid N in Figure 6(a), and $\{2, 3, 4\}$ while searching from destination grid B to the target grid N. Suppose the clockwise angle from line AN to the horizontal direction as A_{AN} . Then the searching directions (P_{ds}) from A to N are defined as Equation (5).

$$P_{ds} = P_{ds} = \{x | x = y \bmod 8, y \in \{z-1, z, z+1\}, z = \lfloor A_{AN} / 45 \rfloor\} \quad (5)$$

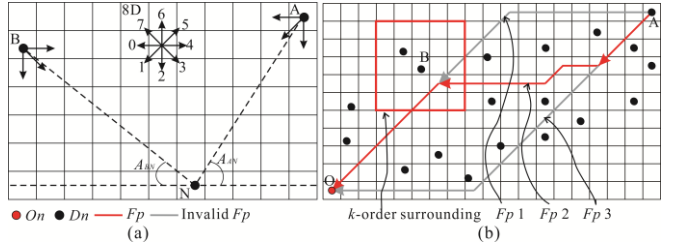


Fig. 6. (a) Definition of searching directions; (b) Definition of searching weights.

(2) Direction weights

Direction weights in a DEM data is usually assigned as the downward slope angle of neighborhood grids defined by their distance and elevation difference [29]. As the mapping space is modelled as a flat surface with DEM, and grids are all with the same elevations. To overcome this problem, the idea according to river system extraction in DEM data that the grid with higher flow accumulation is more likely to be a mainstream is adopted [35]. It means the direction with a larger potential flow accumulation is prior to be explored. The potential flow accumulation (P_f) of each grid is calculated by the total volume of the grids in its k -order surrounding as Equation (6), where f_{ij} is the volume of grid G^{ij} , as shown in Figure 6(b).

$$P_f = \sum_{i=0, j=0}^{i \leq k, j \leq k} f_{ij} \quad (6)$$

The direction weights (S_a) are defined as Equation (7).

$$S_a = \begin{cases} (P_f^c - P_f^n + T_f) / D_{cn} & (P_f^c - P_f^n > 0) \\ T_f / D_{cn} & (P_f^c - P_f^n \leq 0) \end{cases} \quad (7)$$

Where P_f^c and P_f^n are the P_f of two neighborhood grids, T_f is a constant and $T_f \in R^+$ in case $P_f^c - P_f^n \leq 0$, D_{cn} is the distance between two adjacent grids defined as Equation 2. As shown in Figure 6(b), Fp 1 or Fp 3 may be obtained without consideration of P_f with the MSA. While Fp 2 is obtained with consideration of P_f , and Fp 2 is with the same length to Fp 1 or Fp 3. It is clear in the Figure 6(b) that more destinations grids are more likely to connect Fp 2 with shorter paths than to connect Fp 1 or Fp 3 (GC_1). Thus, it can help minimize the total path length of the flow map with the definition.

(3) Searching range refinements considering constraints RC_2 and RC_3

The improved MSA is performed by searching grids with defined directions in searching range to obtained the shortest path between two grids. If certain grids are excluded from the searching range in execution of the improved MSA, the path obtained between two grids by the MSA will never cross the certain grids. Constraints including RC_2 and RC_3 are considered in definition of searching range.

Consideration of RC_2 : RC_2 rules that edge crossings need to be avoided. Suppose the already generated paths as $FpS = \{Fp_1, Fp_2, \dots, Fp_n\}$. When a path between two grids is trying to be obtained with the improved MSA, the grids of $Fp_n \in FpS$ except these two grids are excluded from the searching range. Thus, the path obtained between the two grids will never cross any $Fp_n \in FpS$.

Consideration of RC_3 : RC_3 rules that overlap between paths and nodes needs to be avoided. While obtaining a path from the destination grid to the origin grid with the improved MSA, the k -order surrounding of other destination grids are excluded from the searching range. Thus, the path obtained will never overlap other destination grids.

An example for the improved MSA to obtain the shortest path from destination grid A to the origin grid O is shown in Figure 7. While a path from a destination grid A to the origin grid O is trying to be obtained with the improved MSA, the grid contains the destination node B is excluded from the searching range. Then the grid contains destination node B will never be visited and no overlap will be made at the grid. The flow path colored red which is away from destination node B can finally be obtained.

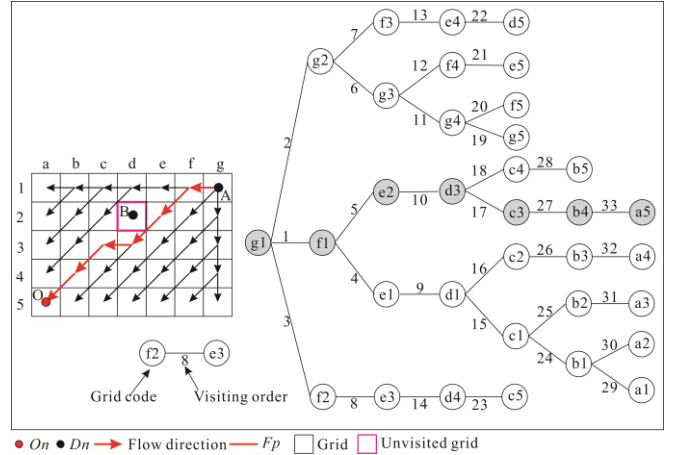


Fig. 7. An example for shortest path calculation with the improved MAS in a DEM data and the searching range definition of the improved MAS.

3.3.3 Path importance

River importance is usually determined by their length and flow volume [35]. As rule by GC_1 , path length may be the first to be considered in a flow map. Thus, the importance of a flow path (FP_{im}) in flow map is defined considering their length. As the paths are generated iteratively, supposed the already generated flow paths as $FpS = \{Fp_1, Fp_2, \dots, Fp_n\}$, a newly generated path from a destination to the origin as Fp_i , Fp_i can be classified into two types according to whether a sub-path of Fp_i is a part of $Fp_n \in FpS$.

Type 1 flow path: no sub-path of Fp_i is a part of $Fp_n \in FpS$.

Type 2 flow path: at least one sub-path of Fp_i is a part of $Fp_n \in FpS$.

If Fp_i is a Type 1 path, it means the path from the destination grid straightly connect to the origin grid which won't flow into any existed $Fp_n \in FpS$. It is more likely to be another mainstream according to the generation process of river system in DEM [35]. Thus, a Type 1 path is more important than Type 2 path. Path importance (FP_{im}) is defined as Equation (8).

$$FP_{im} = \begin{cases} PL_i + G_{im} & (\text{Type 1 Path}) \\ PL_i & (\text{Type 2 Path}) \end{cases} \quad (8)$$

Where G_{im} is a large constant to make sure that Type 1 path is more important than Type 2 path, and $G_{im} = 10000R_s$ in this approach.

3.3.4 Iterative process for flow direction calculation

Given origin grid (OG_1) and destination grids (DG_n) as $GS = \{DG_1, \dots, DG_n\}$ in modelling DEM data according to Section 3.1, the flow paths from all destination grids to the origin grid are generated iteratively as the algorithm in Table 1.

Table 1. Algorithm for flow direction calculation.

Input: Origin grid as OG_1 , destination grids as $GS = \{DG_1, \dots, DG_n\}$ and the DEM data representing the mapping space.
Output: Flow paths from $DG_n \in GS$ to OG_1 as $FpS = \{Fp_1, Fp_2, \dots, Fp_n\}$
Initialization: the output flow paths as $FpS = Null$, the grids of FpS as $FpGS = Null$, and the cache flow paths as $CacheFpS_1 = Null$ and

$CacheFpS_2 = \text{Null}$;

While $GS \text{ Not Null}$ **Do**:

Set $CacheFpS_1 = \text{Null}$;

Foreach $DG_m \in GS$ **Do**:

Set $CacheFpS_2 = \text{Null}$;

Foreach $G_k \in FGS$ **Do**:

Get flow path (Fp_i) with the shortest 'path length' from DG_m to OG_1 which flows in the $Fp_n \in FpS$ or OG_1 at grid G_m with 'improved MSA'; add Fp_i to $CacheFpS_2$;

Get $Fp_j \in CacheFpS_2$ with the shortest 'path length' and add it to $CacheFpS_1$;

Get $Fp_l \in CacheFpS_1$ with the largest 'path importance' and add it to FpS , remove the corresponding destination grid of Fp_l from GS

Return FpS

3.4 Step 3: Flow render based on flow accumulation

(1) Flow accumulation

Flow accumulation of each grid can be generated based on the flow directions. As shown in Figure 8(a), the flow accumulation of a certain grid is the total amount of the flows which gather and pass the grid. The flow accumulation of the origin grid is the total amount of all the outflow of the destinations.

(2) Widths of the flow path

Edges of the flow map need to be rendered with varied widths to delineate the flow volumes. The flow accumulation of each grid has been obtained with the flow accumulation. Thus, width of edges can then be easily rendered based on the accumulation. Suppose the flow accumulation of the origin grid is FV_{sum} , the maximum width is W_{max} , the minimum width as 0.1mm according to human visual resolution [46]. The width (W_i) of an edge with a flow volume as FV_i is defined as Equation (9) with a trigonometric transformation for a smoother change in widths with the increase of FV_i . Rendered result is shown as Figure 8(b).

$$W_i = \sin\left(\frac{FV_i}{FV_{sum}} * \frac{\pi}{2}\right) * (W_{max} - W_{min}) + W_{min} \quad (9)$$

(3) Smooth the flow paths

To further improve the appearance of the flow map, users may tend to render the edges with smooth lines. In this approach, we use the Bézier curve to create smooth paths according to Sun et al. [13], as shown in Figure 8(c).

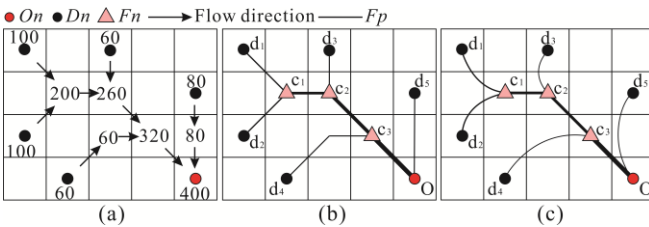


Fig. 8. Flow render based on flow accumulation. (a) Flow accumulation; (b) Flow render with varied widths according to their volume; (c) Smooth the flow paths.

4 EXPERIMENTS

4.1 Result, evaluation and comparison

(1) Data and parameter setting

In this paper, we take the population migrations from Texas to other states in 2000 US Census as experiment data, which has been a widely used benchmark data for flow map production [47]. Data source as: <https://www.ipums.org/>. Parameters are set as follows: $\omega=0.65$ in Equation (3), $k=4$ in Equation (6), $T_d=120^\circ$ for RC_1 , $T_d=\sqrt{2}R_s$ for DC_1 and $k=0$ for RC_3 . The result of the generated flow maps is shown in Figure 9(a), (b) and (c).

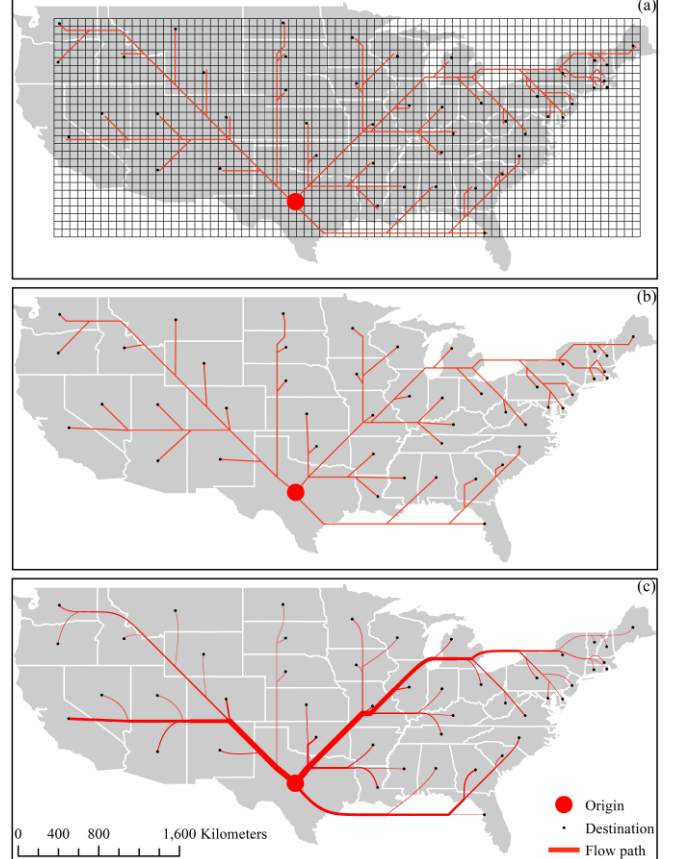


Fig. 9. Flow map for population migration from Texas to other states in 2000 US Census. (a) Flow directions obtained based on the model DEM data; (b) Flow paths; (c) Flow map: the flow paths are smoothed and rendered with varied widths.

(2) Evaluation

The data quality is evaluated according to the quality constraints illustrated in Section 2.1.2 by following measures: total length of the flow map (TL), length of He (EL , minimum EL denoted as EL_{min} , He is defined in Section 2.1.1), acute Fa count (C_{aa} , Fa is defined in Section 3.3.2), edges crossing count (C_{pc}) and overlap count between nodes and paths (C_o). The statistic results are shown as Table 2 and Figure 10.

From Figures 9, 10 and Table 2, we have the following observations: (1) All paths are rendered with varied widths according to their volumes, and they are smoothed based on Bézier curve which are curved ones (GC_1 and DC_3 are satisfied). (2) The distribution of EL in Figure 10 indicates that most EL s are within $[100, 500]$, no EL is very large or small; the coefficient of variation (Cv) for EL is 47.9%, in which $Cv = Std/M * 100\%$, M denotes the average value, and Std denotes the standard

deviation. These denote the EL s are uniform (DC_1 is satisfied) [48]. (3) No acute Fa are made (RC_1 is satisfied); (4) No edges crossings are made (RC_2 is satisfied); (5) No overlap between node and paths are made (RC_3 is satisfied).

Thus, the flow map generated with our approach can well satisfied the defined quality constraints in Section 2.1.2. The parameters to control these quality constraints including T_a and T_d can also be set by users, which will be discussed in Section 4.4.

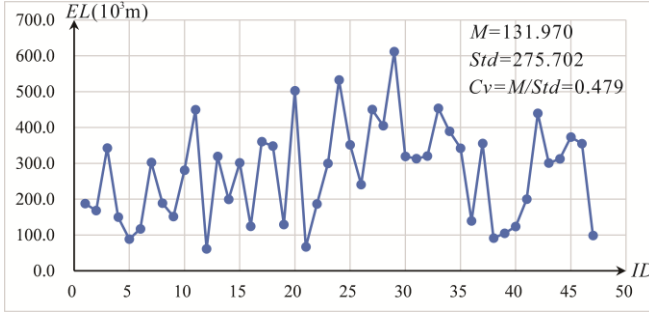


Fig. 10. Distribution of EL s.

(3) Comparisons

To validate the feasibility and generalization ability of proposed approach, we compared the obtained flow maps with proposed approach to existing approaches using triangulation, approximate Steiner trees and path smooth (TNSS) [13], spiral tree (ST) [2], stub bundling strategy (SB) [14] and directed forces (DF) [15], results are shown in Table 2. From Table 2, we have the following observations: (1) A smaller TL can be obtained with our approach by comparing to TNSS, but also close to other approaches with the largest difference by comparing to ST as 3.2; and the result obtained by proposed approach also has the largest EL_{min} , and number of the edges with smaller length ($EL < 100, 70, 40$ and 20) is also the smallest by comparing to other approaches. These indicates a more uniform distribution of flow map can be obtained with total length minimized by proposed approach. (2) No acute Fa , no edge crossing and no overlap between node and paths are made by proposed approach; But TNSS and FD made 4 and 1 acute Fa s, FD made an overlap between node and paths; these indicate that less visual clutter will be made with proposed approach by comparing to the existing approaches.

Table 2. Comparison results obtained based on proposed approach and other approaches.

Measures	RFDA-FM	TNSS	ST	SB	FD
TL (10^6m) ↓	25.2	25.6	22.0	24.5	23.6
EL (10^3m)					
EL_{min} ↑	61.5	27	49.7	13.0	7.8
$n(EL < 100)$ ↓	5	6	27	28	29
$n(EL < 70)$ ↓	2	5	14	17	27
$n(EL < 40)$ ↓	0	3	0	10	5
$n(EL < 20)$ ↓	0	0	0	1	1
$C_{int} (< 120^\circ)$ ↓	0	4	0	0	1

C_{pc} ↓	0	0	0	0	0
C_o ↓	0	0	0	0	1

4.2 Extensions

In above experiments, mapping space is considered as being homogeneous. But mapping space with obstacle areas or heterogeneous mapping space are also widely used in practices. As illustrated in Section 3.2, our approach can also be applicable for these two kinds of mapping space.

Case 1. Mapping space with obstacle areas

Population migration from California to other states in 2000 US Census is taken as experiment data, in which the Great Salt Lake and part of Mississippi river are taken as obstacle areas, Area A and Area B in Figure 11 [47]. Data source as <https://www.ipums.org/>; parameter settings are the same as Section 4.1. Results are shown in Figure 11 and Table 3: The flow maps generated with our approach can well satisfied the defined quality constraints in Section 2.1.2. Compared to the flow map generated by proposed approach without consideration of obstacle areas in Figure 11(a), the total length of the generated flow map in Figure 11(b) by proposed approach only increases 1.9×10^6m (7.53%) if obstacle areas are considered. And the obstacle areas are successfully avoided.

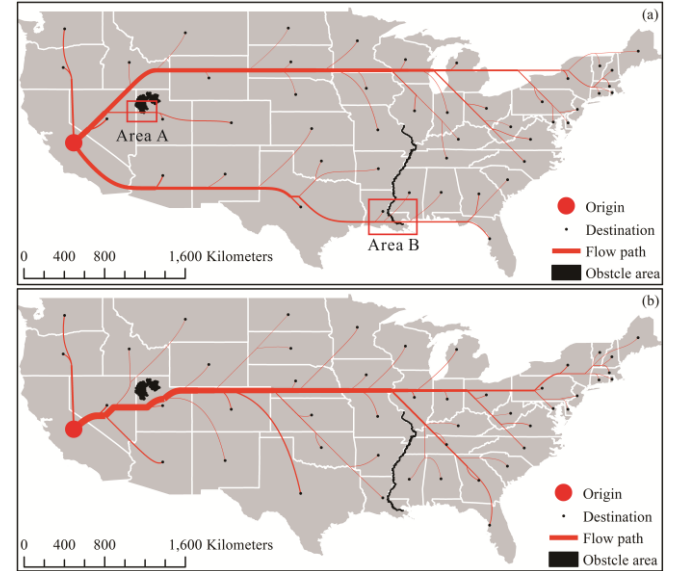


Fig. 11. Flow map for population migration from California to other states in 2000 US Census. (a) Without consideration of obstacle areas; (b) With consideration of obstacle areas.

Case 2. Heterogeneous mapping space

Exports of goods from Russia to other European countries ($\geq 0.01\%$) in 2019 is taken as experiment data, in which sea areas need to be avoided as much as possible to save the transporting expenses, data source as: <https://globaledege.msu.edu/countries/russia/tradestats/>; parameter setting are the same as Section 4.1. To avoid sea areas as much as possible, the resolution of the grids in sea area (SR_s) is set as $SR_s = 1/3 * R_s$ (R_s is defined in Equation (1)). In the improved MSA, the mapping space is searched grid by grid. If a smaller R_s is set for the sea

areas, it means more steps are cost if searching across sea areas. Thus, sea areas can be avoided for the flow map as much as possible. Results are shown in Figure 12 and Table 3: The flow maps generated with our approach can well satisfied the defined quality constraints in Section 2.1.2. And compared to Figure 12(a) and (b) in Area A, B, C, D and E, the flow paths across the sea areas can effectively be avoided.

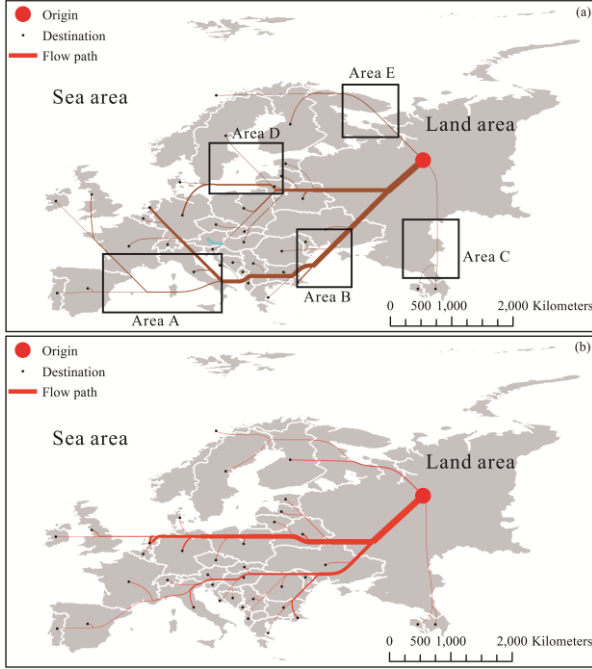


Fig. 12. Flow map for exports of goods from Russia to other European countries ($\geq 0.01\%$) in 2019. (a) Sea areas are not considered; (b) Sea areas need to be avoided as much as possible.

Table 3. Statistics results for the flow maps in different mapping spaces generated by proposed approach.

Measures	Obstacle areas		Mapping space	
	Without	With	Heterogeneous	Homogeneous
$TL (10^6 m) \downarrow$	25.2	27.1	27.8	31.1
$EL (10^3 m)$				
$EL_{min} \uparrow$	71.4	85.1	49.1	79.0
$n(EL < 100) \downarrow$	4	3	4	2
$n(EL < 70) \downarrow$	0	0	1	0
$n(EL < 40) \downarrow$	0	0	0	0
$n(EL < 20) \downarrow$	0	0	0	0
$C_{aa} (< 120^\circ) \downarrow$	0	0	1	0
$C_{pc} \downarrow$	0	0	0	0
$C_o \downarrow$	0	0	0	0

4.3 Ablation experiments

We summarize the strategies applied in proposed approach, e.g., refinements considering quality constraints in Section 2.1.2. These strategies are summarized as Table 4. To validate the feasibility and adaptability of these strategies, the ablation experiments are also performed. Our approach without the different strategies in Table 4 are separately applied for population migrations from Texas to other states in 2000 US Census, and results are shown as Table 5.

Table 4. Strategies applied in our approach.

Name	Descriptions	Location
St_1	The refinement considering RC_1 .	Section 3.3.2
St_2	The refinement considering DC_1 .	Section 3.3.2
St_3	The searching directions in the improved MSA are restricted by Equation (5).	Section 3.3.3
St_4	The searching weights are defined by considering potential flow accumulation.	Section 3.3.3
St_5	The refinement considering RC_2 .	Section 3.3.3
St_6	The refinement considering RC_3 .	Section 3.3.3
St_7	Path importance is defined by considering Type 1 flow path first.	Section 3.3.4

Compared to Table 3 and Table 5, we can see that: (1) The difference (C_v) of EL will increase if any strategy in Table 4 is not performed in proposed approach, especially for St_4 and St_5 ; (2) The EL_{min} will decrease if St_2 , St_3 , St_4 , St_5 and St_6 are not performed in proposed approach; (3) TL of the flow map will increase if St_3 and St_4 are not performed in proposed approach; (4) If the proposed approach is performed without St_1 , 2 acute Fa are made; (5) If the proposed approach is performed without St_6 , 6 overlaps are made between the nodes and the paths. Thus, the 7 strategies in Table 4 performed in proposed approach are proved to be effective.

Table 5. Results of our approach without different strategies listed in Table 4.

Measures	St_1	St_2	St_3	St_4	St_5	St_6	St_7
$TL (10^6 m) \downarrow$	25.0	25.0	25.3	26.1	24.7	24.3	24.7
$EL (10^3 m)$							
$EL_{min} \uparrow$	61.5	39.1	50.7	57.7	57.7	0	61.5
$n(EL < 100) \downarrow$	5	7	5	5	5	7	6
$n(EL < 70) \downarrow$	1	3	3	2	2	6	2
$n(EL < 40) \downarrow$	0	1	0	0	0	6	0
$n(EL < 20) \downarrow$	0	0	0	0	0	6	0
$C_v(\%) \downarrow$	51.8	53.5	49.3	61.7	68.9	58.2	55.3
$C_{aa} (< 120^\circ) \downarrow$	2	0	0	0	0	0	0
$C_{pc} \downarrow$	0	0	0	0	0	0	0
$C_o \downarrow$	0	0	0	0	0	6	0

4.4 Parameter analysis

In this section, we analyze the influence of the parameter settings in proposed approach on the results.

(1) ω in Equation (3)

ω is used to define the path length from a destination node to the origin node. If a small ω is set ($\omega=0.35$), paths from the destination nodes tend to flow in nearby paths, Figure 13(a); while a large ω is set ($\omega=1.0$), paths from the destination nodes tend to flow in a location which is near to the origin node, Figure 13(b). And TL of the flow map will increase with the increase of ω : $TL = 22.8$ for $\omega=0.35$, $TL = 25.2$ for $\omega=0.65$ and $TL = 41.8$ for $\omega=1.0$. But C_v will increase if ω is small or large, $C_v = 57.1\%$ for $\omega=0.35$, $C_v = 47.9\%$ for $\omega=0.65$ and $C_v = 123.79\%$ for $\omega=1.0$. Thus, $\omega=0.65$ is recommended in practice for TL and C_v are within accepted range.

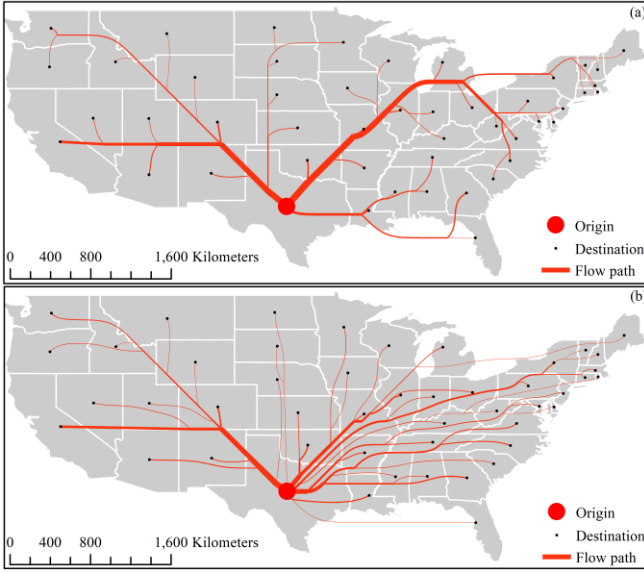


Fig. 13. Flow maps for population migration from Texas to other states in 2000 US Census. (a) $\omega=0.35$; (b) $\omega=1.0$.

(2) k in Equation (6)

k defines the k -order surrounding of the grid, which is used for computation of potential flow accumulation. And the directions with a high potential flow accumulation are prior to be searched in the improved MSA, which helps to minimize the TL of the flow map and obtain a uniform distribution of EL . As shown in Figure 14(a) and (b), if $k=0$ (small k) or $k=8$ (large k), the TL and Cv of the EL will increase as $TL=26.1$, $Cv=61.7\%$ for $k=0$ and $TL=25.9$, $Cv=71.3\%$ for $k=8$. While $k=4$, $TL=25.2$ and $Cv=47.9\%$ are the smallest. In practices, $k=4$ is recommended.

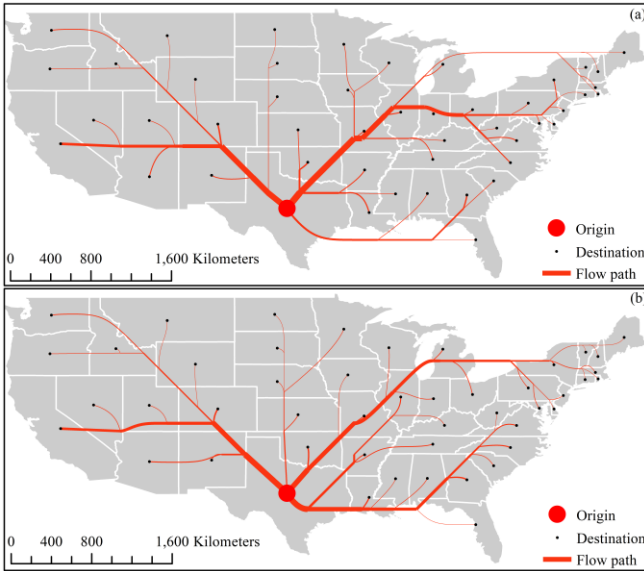


Fig. 14. Flow maps for population migration from Texas to other states in 2000 US Census. (a) $k=0$; (b) $k=8$.

(3) T_a for RC_1

T_a is used to avoid acute Fa . If $T_a=90^\circ$, result is shown as Figure 15. A smaller T_a means a loosen constraint for RC_1 , the TL of the flow map will decrease as $25.0 \times 10^6 m$, reduce $0.2 \times 10^6 m$ (0.79%) by comparing to Figure 9(c). But a smaller T_a also means acute Fa will be made, e.g., two acute Fas are made in Area A and B in Figure 15 if

$T_a=90^\circ$. In practice, $T_a=120^\circ$ is recommended.

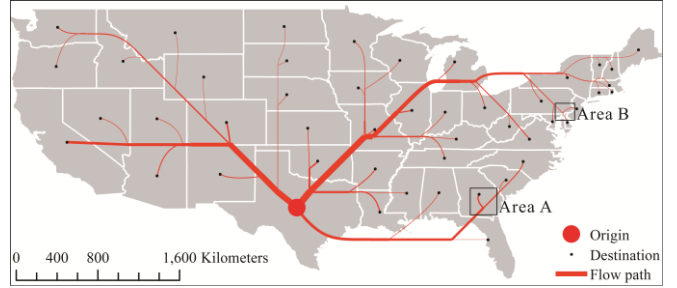


Fig. 15. Flow maps for population migration from Texas to other states in 2000 US Census with $T_a=90^\circ$.

(4) T_d for DC_1

T_d is used to avoid small EL which help obtain a uniform distribution of EL , as shown in Figure 16(a) and (b), the EL can most be controlled within setting parameters ($T_d=R_s$ and $T_d=3 \times R_s$). But a larger T_d means the constraint is harder to be met. As the flow map with proposed approach is obtained with an iterative process, some unexpected results violate the constraint may also be obtained, e.g., short Hes in Area A and Area B in Figure 16(b) with $T_d=3 \times R_s$. The strategies to improve the results are discussed in Section 4.5. As a satisfied result can successfully be obtained with $T_d=\sqrt{2} \times R_s$ and the EL_{min} is smaller than all the previous approaches, and $T_d=\sqrt{2} \times R_s$ is recommended in practice.

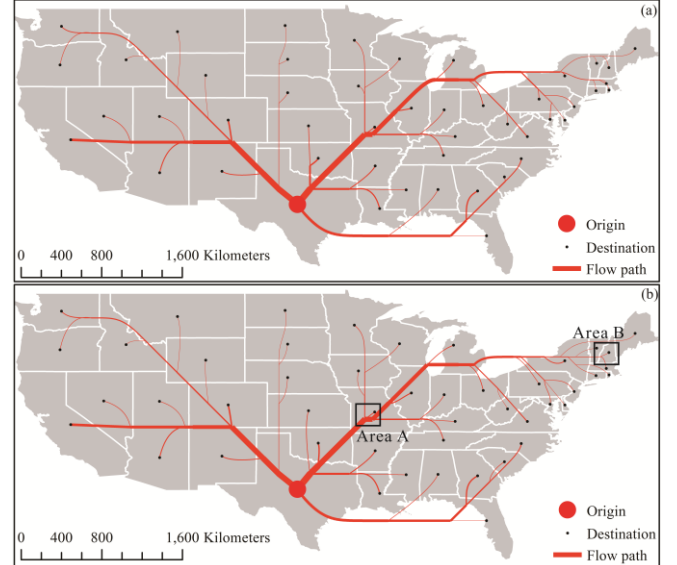


Fig. 16. Flow maps for population migration from Texas to other states in 2000 US Census. (a) $T_d=R_s$; (b) $T_d=3 \times R_s$.

(5) Other parameters

Some other parameters such as the resolution (R_s) of the modelling DEM data, default priority of searching direction in the improved MSA may also need to be set in proposed approach. These parameters are set as default according to previous works. For example, large R_s will lead to an error because the closest points may fall into the same grid; while a small R_s may increase the computational cost. And R_s is set as Equation (1) according to Hengl [43]. These parameters can also be set according to

user demands.

4.5 Discussion

Although satisfied flow maps in different kinds mapping spaces can be generated by using proposed approach with defined quality constraints in Section 2.1.2 satisfied, and the constraints can be controlled with setting parameters. Proposed approach also has some limitations.

(1) As the flow paths are generated with an iterative process by an improved MSA. Thus, a result which meets the quality constraints as much as possible is just obtained each time, but not an optimal one. Sometimes, we may obtain some unexpected results, e.g., short edges in Area A and B in Figure 16(b). The result can be improved in our approach. As illustrated in Section 3.3.3, a k -order surrounding of the destination node refinement is adopted for RC_3 , and $k=0$ is set in proposed approach. As shown in Figure 16(b), if a larger k is set for the target destination nodes which connect short edges, then the result can be improved. Furthermore, a backtracking strategy can also be applied if defined unexpected results occur.

(2) Though the heterogeneous mapping space is considered in our approach, but nodes of the mapping data may also distribute heterogeneously in the mapping space. The heterogeneous distribution of mapping data is not well considered in proposed approach, e.g., the destination nodes of mapping data may with varied densities in different areas. Though a k -order surrounding is considered in definition of the potential flow accumulation and refinement of RC_3 , the k -order surrounding may need to be adapted to the varied density. For example, if an adaptive k -order surrounding is adopted for refinement of RC_3 , the unexpected results in Figure 16(b) can also be avoided.

(3) The proposed approach focuses to map data with one origin to many destinations. But in practice, data with multiple origins to many destinations or many origins to many destinations are also commonly used data, our approach needs to be extended for these data in future works.

(4) The generation of the flow map for the experiment data with 1 origin and 46 destinations will cost 6 minutes with proposed approach. Though an approximate approach is also provided to reduce the searching space in our uploaded code which can shorten the time within 1 minute. More efficient strategies to speed up the proposed approach may need to be provided. Many efficient strategies have been introduced in DEM data processing, and these strategies can also be applied in our approach.

5 CONCLUSION

To generate a flow map for visualization of movement data over time and across space, a river flow directions assignment algorithm over flat surfaces in DEM is applied after the mapping space is modelled as a DEM data. Experiments shows that flow map layout obtained by proposed approach can have a higher

quality on uniform distribution of edge lengths and avoidance of self-intersections and acute angles by comparing to the existing approaches. Furthermore, the experiments demonstrate that our approach is also applicable for heterogeneous mapping space and mapping space with obstacle area. Besides, all the quality constraints can be controlled with setting parameters by users.

Future works will focus on: (1) Adaptive algorithm for different distributions of mapping data; (2) Visualization of flow map with multiple origins and dynamic data; (3) Improvement of algorithm efficiency.

ACKNOWLEDGMENT

We wish to thank our collaborators, Su Ding, Yang Wang, Yuanben Zhang and Wenjia Xu for their time and expertise. The authors wish to thank Tingzhong Huang for his help in data collection. This work was supported in part by a grant from The National Natural Science Foundation of China (No.41871378).

REFERENCES

- [1] A. H. Robinson. The 1837 maps of Henry Drury Harness. *The Geographical Journal*, 121(4): pp.440–450, 1955.
- [2] K. Buchin, B. Speckmann, and K. Verbeek. Flow map layout via spiral trees. *IEEE transactions on visualization and computer graphics*, 17(12), 2536–2544, 2011.
- [3] M. Castells and C. Blackwell. The information age: economy, society and culture. Volume 1. The rise of the network society. *Environment and Planning B: Planning and Design*, 25, 631–636, 1998.
- [4] S. Schöttler, Y. Yang, H. Pfister and B. Bach. Visualizing and interacting with geospatial networks: A survey and design space//*Computer Graphics Forum*. 2021.
- [5] D. Guo and X. Zhu. Origin-destination flow data smoothing and mapping. *IEEE Transactions on Visualization and Computer Graphics*, 20(12): 2043–2052, 2014.
- [6] Y. Yang, T. Dwyer, B. Jenny, K. Marriott, M. Cordeil and H. Chen. Origin-destination flow maps in immersive environments. *IEEE transactions on visualization and computer graphics*, 25(1): 693–703, 2018.
- [7] D. Phan, L. Xiao, R. Yeh and P. Hanrahan. Flow map layout. *IEEE Symposium on Information Visualization (INFOVIS 2005)*. IEEE, 219–224, 2005.
- [8] H. Zhou, P. Xu, X. Yuan and H. Qu. Edge bundling in information visualization. *Tsinghua Science and Technology*, 18(2): 145–156, 2013.
- [9] B. Jenny, D. M. Stephen, I. Muehlenhaus, B. E. Marston, R. Sharma, E. Zhang and H. Jenny. Force directed layout of origin-destination flow maps. *International Journal of Geographical Information Science*, 31(8), 1521–1540, 2017.
- [10] J. Wood, J. Dykes and A. Slingsby. Visualisation of origins, destinations and flows with OD maps. *The Cartographic Journal*, 47(2), 117–129, 2010.
- [11] X. Zhu and D. Guo. Mapping large spatial flow data with hierarchical clustering. *Transactions in GIS*, 18(3), 421–435, 2014.
- [12] Y. Yang, T. Dwyer, S. Goodwin and K. Marriott. Many-to-many geographically-embedded flow visualisation: An evaluation.

- IEEE transactions on visualization and computer graphics*, 23(1): 411–420, 2016.
- [13] S. Sun. A spatial one-to-many flow layout algorithm using triangulation, approximate Steiner trees, and path smoothing. *Cartography and Geographic Information Science*, 46(3): 243–259, 2019.
 - [14] A. Nocaj and U. Brandes. Stub bundling and confluent spirals for geographic networks. *International Symposium on Graph Drawing*. Springer, Cham: 388–399, 2013.
 - [15] A. Debiasi, B. Simões and R. De Amicis. Force directed flow map layout. *2014 International Conference on Information Visualization Theory and Applications (IVAPP)*. IEEE, 170–177, 2014.
 - [16] L. Wang, T. Ai, Y. Shen and J. Li. The isotropic organization of DEM structure and extraction of valley lines using hexagonal grid. *Transactions in GIS*, 24(2): 483–507, 2020.
 - [17] B. Jenny, D. M. Stephen, I. Muehlenhaus, B. E. Marston, R. Sharma, E. Zhang and H. Jenny. Design principles for origin-destination flow maps. *Cartography and Geographic Information Science*, 45(1): 62–75, 2018.
 - [18] W. Dong, S. Wang, Y. Chen and L. Meng. Using eye tracking to evaluate the usability of flow maps. *ISPRS International Journal of Geo-Information*, 7(7): 281, 2018.
 - [19] C. Bennett, J. Ryall, L. Spalteholz and A. Gooch. The aesthetics of graph visualization. In D. W. Cunningham, G. Meyer, & L. Neumann (Eds), *Computational Aesthetics'07: Proceedings of the Third Eurographics conference on Computational Aesthetics in Graphics, Visualization and Imaging* (pp. 57–74). Aire, 2007.
 - [20] C. Ware, H. Purchase, L. Colpoys and M. McGill. Cognitive measurements of graph aesthetics. *Information Visualization*, 1(2), 103–110, 2002.
 - [21] W. Huang, S. H. Hong and P. Eades. Effects of crossing angles. *Paper presented at the Visualization Symposium, PacificVIS '08*. IEEE Pacific, Kyoto, 2008.
 - [22] W. Huang, P. Eades and S. H. Hong. Larger crossing angles make graphs easier to read. *Journal of Visual Languages & Computing*, 25(4), 452–465, 2014.
 - [23] D. Holten and J. J. van Wijk. A user study on visualizing directed edges in graphs. *Paper presented at the CHI '09 SIGCHI Conference on Human Factors in Computing Systems*, Boston, 2009.
 - [24] A. H. Robinson. Early thematic mapping in the history of cartography. *University of Chicago Press*, Chicago, 1982.
 - [25] W. R. Tobler. Experiments In Migration Mapping By Computer. *Cartography and Geographic Information Science*, 14(2):155–163, 1987.
 - [26] S. van den Elzen and J. J. van Wijk. Multivariate network exploration and presentation: From detail to overview via selections and aggregations. *IEEE Transactions on Visualization and Computer Graphics*, 20(12):2310–2319, 2014.
 - [27] K. Buchin, B. Speckmann and K. Verbeek. Angle restricted Steiner arborescences for flow map layout. *Algorithmica*, 72(2), 656–685, 2015.
 - [28] S. K. Jensen and J. O. Domingue. Extracting topographic structure from digital elevation data for geographic information system analysis. *Photogrammetric engineering and remote sensing*. 54, 1593–1600, 1988.
 - [29] J. Garbrecht and L. W. Martz. The assignment of drainage direction over flat surfaces in raster digital elevation models. *Journal of hydrology*. 193, 204–213, 1997.
 - [30] P. Soille, J. Vogt and R. Colombo. Carving and adaptive drainage enforcement of grid digital elevation models. *Water resources research*. 39, 1366, 2003.
 - [31] H. Zhang and G. Huang. Building channel networks for flat regions in digital elevation models. *Hydrological Processes: An International Journal*. 23, 2879–2887, 2009.
 - [32] R. Barnes, C. Lehman and D. Mulla. An efficient assignment of drainage direction over flat surfaces in raster digital elevation models. *Computers & Geosciences*. 62, 128–135, 2014.
 - [33] X. Liu, N. Wang, J. Shao and X. Chu. An automated processing algorithm for flat areas resulting from DEM filling and interpolation. *ISPRS International Journal of Geo-Information*, 6(11): 376, 2017.
 - [34] A. Tribe. Automated recognition of valley lines and drainage networks from grid digital elevation models: a review and a new method. *Journal of hydrology*. 139, 263–293, 1992.
 - [35] H. Zhang, Z. Yao and Q. Yang, et al. An integrated algorithm to evaluate flow direction and flow accumulation in flat regions of hydrologically corrected DEMs. *Catena*, 151: 174–181, 2017.
 - [36] Q. Zhu, Y. Tian and J. Zhao, J. An efficient depression processing algorithm for hydrologic analysis. *Computers & Geosciences*. 32, 615–623, 2006.
 - [37] L. Wang and H. Liu. An efficient method for identifying and filling surface depressions in digital elevation models for hydrologic analysis and modelling. *International Journal of Geographical Information Science*. 20, 193–213, 2006.
 - [38] R. Barnes, C. Lehman and D. Mulla. Priority-flood: an optimal depression-filling and watershed-labeling algorithm for digital elevation models. *Computers & Geosciences*. 62, 117–127, 2014.
 - [39] C. Su, X. Wang, C. Feng, Z. Huang and X. Zhang. An integrated algorithm for depression filling and assignment of drainage directions over flat surfaces in digital elevation models. *Earth Science Informatics*. 1–11, 2015.
 - [40] C. Su, C. Feng, X. Wang, Z. Huang and X. Zhang. An efficient algorithm for assignment of flow direction over flat surfaces in raster DEMs based on distance transform. *Earth Science Informatics*. 1–9, 2016.
 - [41] W. Yu, C. Su, C. Yu, X. Wang, C. Feng and X. Zhang. An efficient algorithm for depression filling and flat-surface processing in raster DEMs. *IEEE Geoscience and Remote Sensing Letters*. 12, 424–428, 2014.
 - [42] I. Florinsky. Digital terrain analysis in soil science and geology. *Academic Press*, 2016.
 - [43] T. Hengl. Finding the right pixel size. *Computers & geosciences*, 32(9): 1283–1298, 2006.
 - [44] D. M. Willardson. Analysis of micro mouse maze solving algorithm. *Learning From Data*, 2001.
 - [45] J. F. O'Callaghan and D. M. Mark. The extraction of drainage networks from digital elevation data. *Computer Vision, Graphics, & Image Processing*, 28(3), 323–344, 1984.
 - [46] Z. Wei, Y. Liu, L. Cheng and S. Ding. A Progressive and Combined Building Simplification Approach with Local Structure Classification and Backtracking Strategy. *ISPRS International Journal of Geo-Information*, 10(5): 302, 2021.
 - [47] S. Ruggles, S. Flood, S. Foster, R. Goeken, J. Pacas, M. Schouweiler and M. Sobek. IPUMS USA: Version 11.0 [dataset]. Minneapolis, MN: IPUMS, 2021. <https://doi.org/10.18128/D010.V11.0>
 - [48] Z. Wei, Q. Guo, L. Wang and F. Yan. On the spatial distribution of buildings for map generalization. *Cartography and Geographic Information Science*, 45(6): 539–555, 2018.
- ZHIWEI WEI** received a B.S. degree and Ph.D. degrees in GIS from Wuhan University, China, in 2015 and 2020. He is currently an Assistant Professor in Aerospace Information Research Institute, Chinese Academic of Sciences. His research interests include automatic map generalization, automatic map design and spatial data visualization.
- SU DING** received Ph.D. degrees in geography from Wuhan Univer-

sity in 2020. She is currently an assistant professor in the College of Environmental and Resource Sciences, Zhejiang A & F University. Her research interests include geospatial information analysis and modeling, spatial data mining.

YANG WANG received Ph.D. degrees in cartography from the Peking university, China, in 2014. She is currently an Associated Professor and a master advisor Aerospace Information Research Institute, Chinese Academy of Sciences, Beijing, China. Her research interests include analysis and visualization of temporal and geographical information.

YUANBEN ZHANG received the B.S. degree from University of Science and Technology of China, in 2011, and the M.S. degree from the Institute of Electronics, Chinese Academy of Science, Beijing, China, in 2014. He is currently an Assistant Professor with the Aerospace Information Research Institute, Chinese Academy of Sciences, Beijing, China. His research interests include geospatial data mining and visualization analysis.

WENJIA XU received her B.Eng. degree with honors in electrical engineering from Beijing Institute of Technology, China in 2016. She worked as a visiting PhD student at the Max-Planck Institute for Informatics in Saarbrücken, Germany between 2019-2020. She is currently a PhD student at the University of Chinese Academy of Sciences, China. Her research interest includes learning with limited supervision for computer vision tasks, explainable machine learning, and visualization.